Flow Distribution Manifolds

R. A. BAJURA

Associate Professor,
Department of Mechanical
Engineering and Mechanics,
West Virginia University,
Morgantown, West Va.
Mem. ASME

E. H. JONES, JR.

1st Lieutenant, USAF,
Williams AFB, Ariz.
Mem. ASME

Flow distribution in the lateral branches of dividing, combining, reverse, and parallel flow manifold systems is studied both analytically and experimentally. Predictions for the flow rates and pressures in the headers of any of the above four basic manifold configurations are obtained from the solution of two first order differential equations involving the flow rate and the pressure difference across headers (pressure-flow equation set), or by the solution of a second order, nonlinear ordinary differential equation involving the flow rate alone (flow distribution equation). Experimental results are presented for various manifold designs having different lateral/header area ratios, lateral flow resistances, and length/diameter ratios. Good agreement is obtained between the analytical and experimental results. Dimensionless parameters which affect flow distribution are identified and discussed with respect to the generalized coefficients of the analytical model. The present method of analysis is proposed for general application in evaluating the performance of flow distribution systems.

Introduction

A manifold is defined here as a flow channel for which fluid enters or leaves through porous side walls due to the action of a differential pressure. Manifolds commonly used in flow distribution systems can be classified into four categorical types, namely, simple dividing or combining flow manifolds and parallel or reverse flow manifold systems. These manifolds are illustrated by Fig. 1. The parallel and reverse flow systems are combinations of the basic dividing and combining flow manifolds interconnected by lateral branches. In a dividing flow header, the main fluid stream is decelerated due to the loss of fluid through the laterals. Therefore, pressure will rise in the direction of flow if the effects of friction are small as can be demonstrated by applying a frictionless Bernoulli equation to the header flow stream. Frictional effects, however, would cause a decrease of pressure in the flow direction. Therefore, the possibility exists for obtaining a uniform pressure along the dividing flow header by suitable adjustment of the flow parameters so that the pressure regain due to flow branching balances the pressure losses due to friction. The combining flow header is characterized by a falling pressure in the direction of flow. This characteristic occurs due to the additive effects of both the frictional pressure losses and the favorable pressure gradient required for acceleration of the main stream due to the inflow at the branch points. The movement of fluid through the porous wall is governed by a discharge equation for the crossflow stream in which the cross-flow velocity head is related to the pressure differential by a flow (or discharge) coefficient which accounts for frictional losses along the lateral flow path.

If the flow field is considered as one dimensional, the governing equations for the manifold are the continuity and momentum equations for each header and the discharge equation for the lateral flows. Under suitable assumptions, the work-energy equation can also be applied to the header flow stream. The prediction of the performance of a manifold depends on the proper selection of the momentum exchange and the discharge coefficients for the given system and the formulation of a valid physical model for the branching process. The prediction of the lateral flows for a manifold with many branches is accomplished more readily by a continuous flow model as opposed to a discrete branch point model. The objectives of this paper are to present
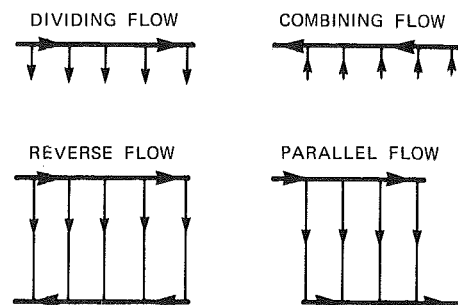
Fig. 1 Four types of manifolds

a valid physical and analytical model applicable to a wide variety of manifold system designs and to illustrate the application of this model to a system of uniform cross-sectional dimensions. The validity of the analytical model is demonstrated for experimental systems studied by the present writers and other investigators.

Literature

Coefficient Data. Earlier discrete branch point analytical models predicted the performance of manifolds by determining the discharge at an individual branch point in terms of some assumed local pressure and flow conditions. The discharges in each lateral were iteratively adjusted until the overall discharge matched the given flow rate for the system. Therefore, the early experimental work concentrated on determining flow coefficients at single, isolated branch points. The major contribution to the data for pressure changes and flow loss coefficients at discrete branch points was made by McNown [1, 2][1] for circular pipes with right angled, sharp-edged junctions between the lateral and the header. Other experimental data have been reported for these geometries by Zeisser [3], Starosolszky [4], Ruus [5], and Kubo and Ueda [6, 7]. Flow coefficients for other lateral geometries, such as simple holes or short tubes, have been determined by Oakey [8], Koh and Brooks [9], Acrivos, Babcock and Pigford [10], Keller [11], Dow [12], and Dittrich [13]. Much of the data for flow coefficients has been obtained for branch points which are infinitely spaced along the header and, therefore, the relevance of this data to situations where branch points are closely spaced is questionable. McNown [1] has shown that the pressure regain characteristics at a branch point are strongly dependent on the spacing between laterals. The geometry of the branch point itself was shown by Zeisser [3] to have no effect on the pressure regain characteristics but to have a profound effect on the flow losses incurred by the branch stream turning into the lateral from the header. The results of Kubo and Ueda [6] illustrate that the flow coefficients may be considered as independent of Reynolds number for a wide flow range.

Analytical Models. The overall analysis of the performance of a manifold system is based primarily on the analytical model chosen to represent the branching process. Considering first the flow stream in the header, the pressure rise in dividing flow (or pressure decrease in combining flow) has been analyzed traditionally by the application of the Bernoulli theorem, the work

energy theorem (First Law), or the conservation of momentum theorem. In applying either the Bernoulli or work-energy equations to the branching process, it was argued that the mechanical energy before branching should be equal to the mechanical energy after branching plus some losses due to friction. However, McNown [1] has shown that the mechanical energy after branching for the dividing flow header can be greater than the approaching energy. This result occurs due to the rearrangement of fluid between the boundary layer and the main stream as the branch point is traversed, such that fluid of low kinetic energy is discharged into the lateral with higher kinetic energy fluid remaining in the header. The apparent violation of the First Law of Thermodynamics (work-energy equation) can be explained by noting that the energies of the three fluid streams are calculated on a per unit mass basis, whereas the energy conservation theorem is based on the overall energy flow rates in the control volume. If the specific mechanical energies of each fluid stream are multiplied by the relevant mass flow rate terms, then the overall mechanical energy of the two fluid streams leaving the dividing flow branch point is shown to be less than the approaching energy flow rate. The loss of mechanical energy is accounted for in the gain in internal energy of the fluid due to viscous dissipation. Therefore the overall work-energy equation is satisfied.

The difficulty with applying a Bernoulli equation to the branching process lies in the ambiguity which exists in identifying a relevant streamline on which to conserve energy and estimate frictional losses. Other authors have avoided this question by applying a momentum equation along the header. Models have been proposed by Enger and Levy [14], Van Der Hegge Zijnen [15], Markland [16], and Acrivos, Babcock and Pigford [10] which relate the pressure changes to the momentum changes in the main flow stream and frictional losses which are based on the local flow speed. In the above flow models, the effects of axial momentum transport by the lateral fluid stream are not considered. In addition, these models have been applied only to the case of simple dividing flow manifolds.

In an earlier paper, Soucek and Zelnick [17] proposed a model for discharge ports in a lock system which included the effect of axial momentum transport by the transverse flow stream. This model was developed by Bajura [18] and applied to both dividing and combining flow manifolds. The flow model proposed by these latter two references is more physically acceptable than the previous models since the overall momentum balance (integral equation) is satisfied for the control volume as a whole and remains valid independent of the effects of friction or the rearrangement of streamlines due to the branching process.

---

[1] Numbers in brackets designate References at end of paper.

Calculational Procedures. Calculational models to evaluate the

---

━━━━━━ Nomenclature ━━━━━━

A = area, friction coefficient

A_r = area ratio

B = momentum coefficient

C_{TC} = turning loss coefficient for combining flow

C_{TD} = turning loss coefficient for dividing flow

D = header diameter

d = lateral diameter, differentiation

f = Moody friction factor

H = lateral resistance coefficient in velocity heads

K = local flow loss coefficient in velocity heads

L = header length

l = lateral length

M = momentum coefficient

N = number of branch points along header

n = friction factor exponent

P = pressure

Q = volume flow rate

T = wall shear stress

V = velocity

x = distance along header

Z = dimensionless discharge coefficient

β = momentum coefficient for header flow

γ = momentum coefficient for lateral flow

Δ = differential between parameters

θ = overall momentum coefficient for header flow

π = perimeter

ρ = density

Φ = friction term

Subscripts and Superscripts

0 = maximum velocity condition

1 = dividing flow header

2 = combining flow header

3 = lateral

x = axial flow

y = transverse flow

$(^-)$ = overbar, average value

$(')$ = differentiation

performance of a manifold system can be formulated from several viewpoints. It is often desired to design a system with balanced flow in each lateral flow stream. Such designs can be accomplished by altering the size of the laterals, their flow resistance, or the cross-sectional area of the duct. These systems have been described by Howland [19] for round pipes, Perlmutter [20] and Mardon, et al. [21] for tapered manifolds, Haerter [22] for air conditioning systems, and Koh and Brooks [9] for ocean outfalls. None of these models considers the loss of axial momentum from the control volume due to the transverse flow. Other computational models approach the design problem from the standpoint of analyzing the performance of a given system. System models of this type are described by Horlock [23] for slotted pipes, Olson [24], Huang and Yu [25], and Quaile and Levy [26] for porous ducts in laminar flow, and Bajura, LeRose and Williams [27] for manifold systems.

In view of the widely scattered values of flow coefficients and the different system geometries, it is clearly recognized that each manifold design must be evaluated based on its own characteristics. However, a generalized method of analysis is required which can be applied to widely different manifold designs and different computational viewpoints. The flow model described in the present document satisfies this need and is proposed as a general model for manifold analysis.

Analytical Model for Manifold Flow

In presenting the analytical model, the authors have chosen a particular design relevant to superheater systems to illustrate the development of the governing equations. In this section, the system model is first defined for discrete branch points and is then applied to parallel and reverse flow superheater systems. The system equations are later developed in a generalized, non-dimensional form which can be applied to each of the four manifolds identified by Fig. 1 by properly defining the relevant parametric groups for the given design.

Basic Equations. Consider first the control volume illustrated by Fig. 2 which describes the flow streams near a dividing flow branch point. The outflow of fluid at surface A_{31} has velocity components V_x and V_y since it is assumed that the discharged fluid has not turned completely 90 degrees when crossing the boundary of the control volume. The length of the control volume in the streamwise direction is Δx_1, which is calculated by

dividing the axial length, L_1, by the total number of branch points, N_1. The lateral area at the branch point, A_{31}, is assumed constant along the header, and the branch points are uniformly distributed. The fluid is assumed to be incompressible and the header area, A_1, is assumed constant. The flow conditions at $(x_1 + \Delta x_1)$ are related to the flow conditions by x_1 by a first order Taylor series expansion. For the control volume of Fig. 2, the continuity equation is written as:

$$\bar{V}_{31}A_{31} = - A_1 \frac{d\bar{V}_1}{dx_1} \frac{L_1}{N_1} \qquad (1)$$

where $\bar{V}_{31}$ and $\bar{V}_1$ are average velocities. Letting P represent the pressure and T_w the wall shear stress, the momentum equation in vector form is written for the control volume as:

$$- \int_{\text{Surface}} P \, \vec{dA} + \int_{\text{Surface}} T_w \, \vec{dA} = \int_{\text{Surface}} \rho \vec{V} \, (\vec{V}d\vec{A}). \qquad (2$$

It is desirable to express the momentum transport in terms of local average velocities. The following parameters are defined: β_1 is an axial flow momentum correction factor, γ_1 is a lateral flow momentum correction factor for axial momentum transport through surface A_{31}, θ_1 is an overall momentum correction factor, π_1 is the perimeter of the header, T_1 is the wall shear stress, f_1 is the Moody friction factor, and P_1 is the pressure. These parameters are formally defined as:

$$\beta_1 = (1/\bar{V}_1^2 A_1) \int_{A_1} V_1^2(A_1) dA_1 \qquad (3)$$

$$\gamma_1 = (1/\bar{V}_1 \bar{V}_{31} A_{21}) \int_{A_{31}} V_x(A_{31}) V_y(A_{31}) dA_{31} \qquad (4)$$

$$\theta_1 = 2\beta_1 - \gamma_1 \qquad (5)$$

$$T_1 = f_1 \rho \bar{V}_1^2/8 \qquad (6)$$

The momentum equation for the dividing flow control volume in terms of the above parameters is:

$$\frac{1}{\rho} \frac{d\bar{P}_1}{dx_1} + \left(\frac{f_1\pi_1}{8A_1} + \frac{d\beta_1}{dx_1} \right) \bar{V}_1^2 + \theta_1 \bar{V}_1 \frac{d\bar{V}_1}{dx_1} = 0 \qquad (7)$$

Fig. 3 illustrates control volumes for the analysis of combining flow headers. Fig. 3(a) shows the flow direction pertinent to a reverse flow manifold system. Using an analysis similar to the dividing flow header above, the momentum equation is:

$$\frac{1}{\rho} \frac{d\bar{P}_2}{dx_2} + \left(- \frac{f_2\pi_2}{8A_2} + \frac{d\beta_2}{dx_2} \right) \bar{V}_2^2 + \theta_2 \bar{V}_2 \frac{d\bar{V}_2}{dx_2} = 0 \qquad (8)$$

where θ_2 is defined as $(2\beta_2 - \gamma_2)$ in an analogous fashion with equation (5). The sign of the friction term is negative in equation (8) since the flow direction is defined as being positive in the negative x_2 direction. Fig. 3(b) illustrates the control volume for the combining flow header of a parallel flow manifold system. The momentum equation for this configuration is:

$$\frac{1}{\rho} \frac{d\bar{P}_2}{dx_2} + \left(\frac{f_2\pi_2}{8A_2} + \frac{d\beta_2}{dx_2} \right) \bar{V}_2^2 + \theta_2 \bar{V}_2 \frac{d\bar{V}_2}{dx_2} = 0 \qquad (9)$$

At this stage in the analysis, there are four unknowns, namely, the pressures $\bar{P}_1$ and $\bar{P}_2$, and the velocities $\bar{V}_1$ and $\bar{V}_2$. The velocities are related by inter-manifold continuity equations which ensure that the flow from one header enters the other. These inter-manifold continuity equations are:

$$\bar{V}_2 = \bar{V}_1(A_1/A_2) \qquad (10)$$

for the reverse flow manifold system, and

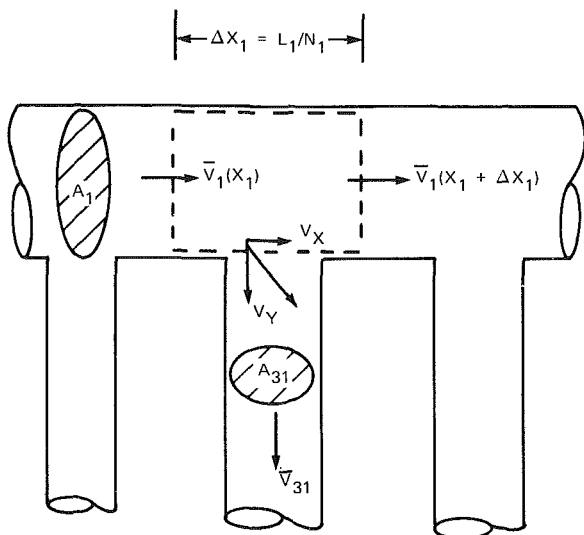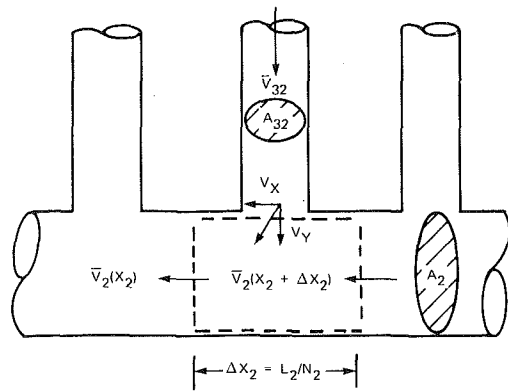$$\bar{V}_2 = (\bar{V}_{10} - \bar{V}_1)(A_1/A_2) \qquad (11)$$

Fig. 2 Dividing flow branch point control volume
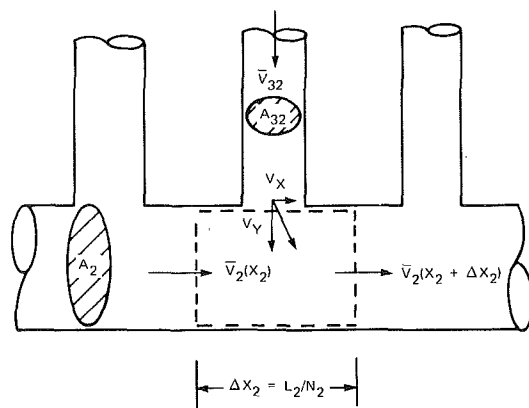
(A) REVERSE FLOW

(B) PARALLEL FLOW

Fig. 3 Combining flow branch point control volume

Fig. 4 Control volume for lateral discharge flow

for the parallel flow manifold system. The term $\bar{V}_{10}$ is the average velocity at the inlet to the dividing flow header. The relationships defined by equations (10) and (11) are valid at correspondingly scaled distances x_1 and x_2 for each header. By employing the inter-manifold continuity relationships, the velocity $\bar{V}_2$ may be eliminated from the equations, leaving only the unknowns of $\bar{P}_1$, $\bar{P}_2$, and $\bar{V}_1$.

A relationship between the pressure differential between manifolds and the lateral flow rate is obtained in terms of a discharge equation written in the following manner with respect to the control volume illustrated by Fig. 4:

$$\frac{\bar{P}_1}{\rho} = \frac{\bar{P}_2}{\rho} + \frac{\bar{V}_{31}^2}{2}\left(\frac{A_{31}}{A_{32}}\right)^2$$

$$+ \frac{\bar{V}_{31}^2}{2}\left[C_{TD} + K_{eq} + (fl/d)_{eq} + C_{TC}\left(\frac{A_{31}}{A_{32}}\right)^2 \right] \quad (12)$$

The term C_{TD} is a turning loss for flow entering the lateral from the dividing flow header; the terms K_{eq} and $(fl/d)_{eq}$ represent the equivalent loss coefficient (based on the velocity $\bar{V}_{31}$) for local upset flow losses and ordinary friction losses; and the term C_{TC} is a turning loss for flow into the combining header. The area ratio term, (A_{31}/A_{32}) is an adjustment to allow for the possibility that the area of the lateral changes from the inlet end to the outlet end. By writing the discharge relation as in equation (12), no credit is taken for any approaching velocity head $(\bar{V}_1^2/2)$
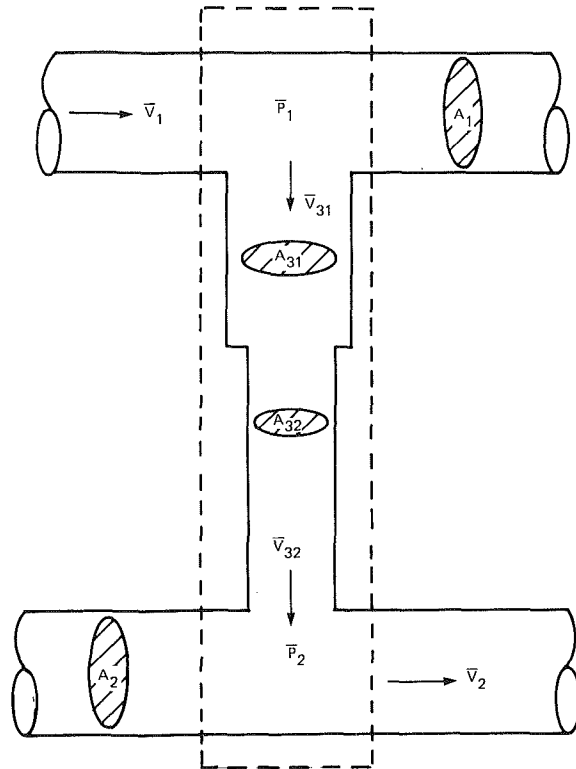
in the dividing flow header. It is assumed that the lateral fluid enters the combining flow header as a stream with velocity $\bar{V}_{32}$ and not the velocity $\bar{V}_2$. Any mixing effects are accounted for in the turning loss term C_{TC}. The lateral flow resistance term, H, is defined in terms of equation (12) as:

$$\frac{\bar{P}_1 - \bar{P}_2}{\rho} = \frac{\Delta \bar{P}_{12}}{\rho} = H\frac{\bar{V}_{31}^2}{2} = \frac{H}{2}\left(-\frac{A_1}{A_{31}}\frac{d\bar{V}_1}{dx_1}\frac{L_1}{N_1} \right)^2 \quad (13)$$

where $\Delta\bar{P}_{12}$ is the differential pressure between headers. When the overall flow resistance, H, becomes large, the turning loss terms assume minor significance in the discharge equation.

Equation (13) may be manipulated to obtain several relationships between the differential pressure and flow rate in the dividing flow header. The first relationship is obtained by solving equations (1) and (13) for the velocity gradient, $d\bar{V}_1/dx_1$, as:

$$\frac{d\bar{V}_1}{dx_1} = -\frac{N_1 A_{31}}{A_1 L_1}\left(\frac{2}{\rho H}\right)^{1/2}(\Delta\bar{P}_{12})^{1/2} \quad (14)$$

The minus sign is chosen since the velocity $\bar{V}_1$ must decrease with distance x_1. This condition also requires that the pressure differential always be positive or a reversal of flow will occur. (This is not to say that a reversal of flow cannot occur in actual systems.) The second relationship between the differential pressure and the flow rate is obtained by differentiating equation (14) and solving for the differential pressure gradient. This result is:

$$\frac{1}{\rho}\frac{d(\Delta\bar{P}_{12})}{dx_1} = H\left(\frac{A_1 L_1}{A_{31} N_1}\right)^2\frac{d\bar{V}_1}{dx_1}\frac{d^2\bar{V}_1}{dx_1^2} \quad (15)$$

Equation (15) will be used later to eliminate the pressure terms from the governing equations.

Nondimensional Equations for Manifolds. The relevant equa-

tions for the analysis of flow in manifolds may be nondimensionalized by the following reference quantities: $\bar{V}_{10}$, the entrance velocity to the dividing flow header; L_1 and L_2, the lengths of each header; and Q_0, the entering flow rate, $\bar{V}_{10}A_1$. The nondimensional variables are defined in Table 1.

Table 1 Nondimensional variables

$x = x_1/L_1 = x_2/L_2$	$Q = \bar{V}_1 A_1/Q_0$
$V = \bar{V}_1/V_{10}$	$\Delta P = \Delta \bar{P}_{12}/\rho \bar{V}_{10}^2$

Reverse Flow Manifolds. It is convenient to focus the development of the governing equations on each manifold system independently. Consider the reverse flow manifold system which is governed by equations (7, 8, 10, and 14). As a first step, subtract equation (8) from equation (7) to eliminate the individual pressures and obtain an equation in terms of the differential pressure, $\Delta \bar{P}_{12} = (\bar{P}_1 - \bar{P}_2)$, between the headers. The velocity $\bar{V}_2$ is eliminated by employing the continuity equation (10). After nondimensionalizing the remaining equations as defined by Table 1, a set of two dimensionless equations involving the velocity V and the differential pressure ΔP is obtained in the form:

$$\frac{dV}{dx} = -\frac{N_1 A_{31}}{A_1}(2/H)^{1/2}(\Delta P)^{1/2} \qquad (16)$$

$$\frac{d(\Delta P)}{dx} = -\left[\frac{f_1 L_1 \pi_1}{8 A_1} + \frac{f_2 L_2 \pi_2}{8 A_2}\left(\frac{A_1}{A_2}\right)^2 + \frac{d\beta_1}{dx} - \frac{d\beta_2}{dx}\right]V^2$$
$$- \left[\theta_1 - \theta_2\left(\frac{A_1}{A_2}\right)^2\right]V\frac{dV}{dx}. \qquad (17)$$

Equations (16) and (17) constitute a coupled set of first order equations called the Pressure-Flow Equations which must satisfy the following boundary conditions. At the entrance, the dimensionless velocity V must equal 1. At the dead end of the manifold, the end wall imposes the physical requirement that the velocity V is 0. This condition requires all the flow to be discharged before the dead end of the manifold is reached. While it is possible to prescribe a pressure boundary condition at the inlet, the inlet pressure cannot be specified arbitrarily since the entrance pressure level controls the discharge from the header. Therefore, the pressure at the inlet is intimately tied in with the continuity equation and cannot be specified arbitrarily or the condition of too much or too little discharge will result. The specification of the inlet pressure is equivalent to specifying the derivative, dV/dx, at the inlet [see equation (16)] and would amount to an over-specification of the problem since the boundary values $V(0)$ and $V(1)$, and the derivative $dV/dx(0)$ cannot be specified arbitrarily for a problem which is only of second order.

If the differential pressure is eliminated from equations (16) and (17), a second order equation in the dimensionless flow rate Q can be obtained as:

$$\frac{H}{A_R{}^2}Q'Q'' + \left[\frac{d\beta_1}{dx} - \frac{d\beta_2}{dx}\right]Q^2 + \left[\frac{f_1 L_1 \pi_1}{8 A_1}\right.$$
$$\left. + \frac{f_2 L_2 \pi_2}{8 A_2}\left(\frac{A_1}{A_2}\right)^2\right]Q^2 + \left[\theta_1 - \theta_2\left(\frac{A_1}{A_2}\right)^2\right]QQ' = 0. \qquad (18)$$

The term A_r is called the area ratio of the manifold and is defined as $A_r = N_1 A_{31}/A_1$. Physically, this term is the ratio of the total lateral cross-sectional area to the cross-sectional area of the header.

Equation (18) is a flow distribution equation and is subject to the boundary conditions: $Q(0) = 1$ and $Q(1) = 0$.

Parallel Flow Manifolds. The parallel flow manifold system is described by the dimensional equations (7, 9, 11, and 14). In a

manner similar to the reverse flow system above, the differential pressure is obtained by subtracting equation (9) from equation (7); the inter-manifold continuity equation (11) is used to eliminate the velocity $\bar{V}_2$; and the remaining equations are nondimensionalized with respect to the variables in Table 1. The pressure-flow equation set which results is:

$$\frac{dV}{dx} = -\frac{N_1 A_{31}}{A_1}(2/H)^{1/2}(\Delta P)^{1/2} \qquad (19)$$

$$\frac{d(\Delta P)}{dx} = -\left(\frac{f_1 L_1 \pi_1}{8 A_1} + \frac{d\beta_1}{dx}\right)V^2 + \left(\frac{f_2 L_2 \pi_2}{8 A_2} + \frac{d\beta_2}{dx}\right)*$$
$$\left(\frac{A_1}{A_2}\right)^2 (1 - V)^2 - \theta_1 V\frac{dV}{dx} - \theta_2\left(\frac{A_1}{A_2}\right)^2\frac{dV}{dx}(1 - V). \quad (20)$$

These equations are subject to the boundary conditions $V(0) = 1$ and $V(1) = 0$. If the pressure is eliminated from equations (19) and (20), the resulting flow distribution equation is:

$$\frac{H}{A_R{}^2}Q'Q'' + \left(\frac{f_1 L_1 \pi_1}{8 A_1} + \frac{d\beta_1}{dx}\right)Q^2$$
$$- \left(\frac{f_2 L_2 \pi_2}{8 A_2} + \frac{d\beta_2}{dx}\right)(1 - Q)^2$$
$$+ \theta_1 QQ' + \theta_2(A_1/A_2)^2 Q'(1 - Q) = 0. \qquad (21)$$

This equation is solved subject to the boundary conditions $Q(0) = 1$ and $Q(1) = 0$.

Generalized Equations for Manifold Systems. The previous developments were presented to acquaint the reader with the basic flow model and methods of analysis. The flow distribution in any of the four types of manifolds shown by Fig. 1 can be obtained from the solution of a generalized set of equations given by the following forms:

(i) Pressure-flow equations

$$\frac{dV}{dx} = -Z(\Delta P)^{1/2} \qquad (22)$$

$$\frac{d(\Delta P)}{dx} = -A_1 V^2 + A_2(1 - V)^2 - B_1 V\frac{dV}{dx} - B_2(1 - V)\frac{dV}{dx} \qquad (23)$$

(ii) Flow distribution equation

$$Q'Q'' + \Phi_1 Q^2 + 2\Phi_2 Q + M_1 QQ' + M_2 Q' = \Phi_2 \qquad (24)$$

The definition of the coefficients for the pressure-flow equations is given in Table 2. The coefficients of the flow distribution equation are given in Table 3. Both sets of generalized equations satisfy the boundary conditions:

$$V(0) = Q(0) = 1 \qquad (25)$$

$$V(1) = Q(1) = 0 \qquad (26)$$

The above equations have been formulated under the assumption that the lateral resistance, H, and the distribution of laterals along the headers are constant, i.e., the porosity of the headers is constant. If these parameters vary along the headers, additional terms appear in the flow distribution equation. A discussion of these considerations is given in reference [27].

For many manifold systems, the flow regime is likely to be fully turbulent. For these conditions, the friction factors may be taken as a constant. For smooth surfaces and widely spaced branch points, the friction factor may be a function of the Reynolds number and will vary along the headers due to the changing flow rates. Under these conditions, the friction factors may be assumed to vary as the Reynolds number to a power,

TABLE 2 COEFFICIENTS FOR PRESSURE-FLOW EQUATION SET

Parameter	Dividing Flow	Combining Flow	Reverse Flow	Parallel Flow
ΔP	$\dfrac{\bar{P}_1 - P_{amb}}{\rho \bar{V}_{10}^2}$	$\dfrac{P_{amb} - \bar{P}_2}{\rho \bar{V}_{20}^2}$	$\dfrac{\bar{P}_1 - \bar{P}_2}{\rho \bar{V}_{10}^2}$	$\dfrac{\bar{P}_1 - \bar{P}_2}{\rho \bar{V}_{10}^2}$
V	$\dfrac{V_1}{\bar{V}_{10}}$	$\dfrac{V_2}{\bar{V}_{20}}$	$\dfrac{V_1}{\bar{V}_{10}}$	$\dfrac{V_1}{\bar{V}_{10}}$
A_1	$\dfrac{f_1 L_1}{2D_1}$	$\dfrac{f_2 L_2}{2D_2}$	$\dfrac{f_1 L_1}{2D_1} + \dfrac{f_2 L_2}{2D_2}\left(\dfrac{D_1}{D_2}\right)^4$	$\dfrac{f_1 L_1}{2D_1}$
A_2	0	0	0	$\dfrac{f_2 L_2}{2D_2}\left(\dfrac{D_1}{D_2}\right)^4$
B_1	θ_1	$-\theta_2$	$\theta_1 - \theta_2\left(\dfrac{D_1}{D_2}\right)^4$	θ_1
B_2	0	0	0	$\theta_2\left(\dfrac{D_1}{D_2}\right)^4$
Z	$A_r\sqrt{\dfrac{2}{H}}$	$A_r\sqrt{\dfrac{2}{H}}$	$A_r\sqrt{\dfrac{2}{H}}$	$A_r\sqrt{\dfrac{2}{H}}$

such as $(-1/4)$. If the frictional exponent is given the symbol, n, then the friction factors can be replaced by the expressions:

$$f_1(x) = f_{10}V^{-n} = f_{10}Q^{-n} \tag{27}$$

$$f_2(x) = f_{20}V^{-n} = f_{20}Q^{-n} \tag{28}$$

Where the (0) subscript indicates that the friction factor is evaluated at the maximum Reynolds number for the header. The friction factor is now a function of the flow variable and suitable alteration must be made in the dependent variable terms related to friction for the governing equations.

Experimental Apparatus

A schematic of the experimental apparatus is shown by Fig. 5. The headers and laterals were fabricated from commercial pvc piping materials having diameters of 10.16 cm (4 in.) and 3.81 cm (1.5 in.), respectively. The air flow through the system was induced by connecting the combining flow header outlet to the inlet of a 3.73 kilowatt (5 horsepower) blower. Parallel and reverse flow systems were arranged by capping one of the ends of the dividing flow header. Laterals were attached to the headers by glueing commercial pvc saddles to the headers over holes bored through the side walls. The junction was sharp-edged and was shaped to have a smooth internal diameter with no roughness to disturb the lateral flows. Individual sections of the main headers were joined using commercial pvc couplers which presented a negligible discontinuity to the internal surface of the header. The spacing between branch points was uniform at 2.55 header diameters. Tests were conducted with either 20 or 10 branch points giving header length-to-diameter ratios of 51.0 and 25.5 respectively. The lateral tubes were of uniform diameter and 1.56m (5 ft) in length. Orifices of various internal diameters (0.96, 2.54 and 3.18 cm) were inserted at the midpoint of the laterals to increase the flow resistance.

Each header was instrumented by pressure taps located midway between the branch points and on the opposite side of the header. The static pressures in each header were referenced to the static pressure at either the open or closed end of the header, depending upon the configuration studied as shown by Fig. 5. Differential pressures between headers were measured at the outlet from the combining flow header. The overall flow rate at the entrance to the dividing flow header was measured by a six probe velocity rake using equal area averaging procedures. Flow rates were measured in two laterals using calibrated resistance orifices to monitor the overall flow conditions in the laterals. Reynolds numbers in the headers were of the order of 60,000–80,000 and 8,000–10,000 in the laterals, depending on the manifolds studied. Data for each run were reduced by computer analysis and polynomial curves were fitted to the raw data using a statistical analysis program for use in interpolating routines required to compare the experimental data with the analytical model. The data presented here represents the average of three runs per test case. A more expanded description of the experimental facility and test conditions is given in Jones [28].

Experimental Results

Five configurations were studied experimentally for both parallel and reverse flow manifold systems. The parameters varied were the lateral flow resistance, H, and the relative length, L/D, of the manifold. The number of branch points per manifold was either 10 or 20 depending upon the length of the headers since the spacing between branch points was maintained constant at 2.55 header diameters. One set of experimental runs was carried out for the case of infinite lateral resistance (i.e., constant

TABLE 3 COEFFICIENTS FOR FLOW DISTRIBUTION EQUATION

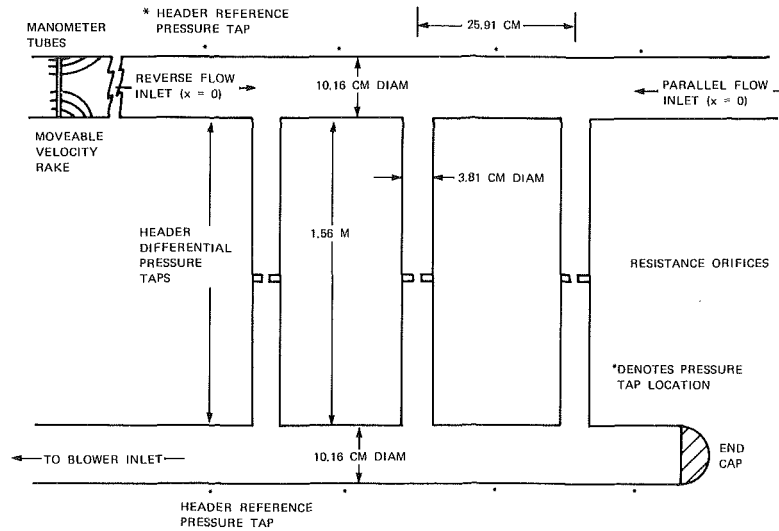| Parameter	Dividing Flow	Combining Flow	Reverse Flow	Parallel Flow
Φ_1	$\dfrac{A_r^2}{H}\dfrac{f_1 L_1}{2D_1}$	$\dfrac{A_r^2}{H}\dfrac{f_2 L_2}{2D_2}$	$\dfrac{A_r^2}{H}\left[\dfrac{f_1 L_1}{2D_1} + \dfrac{f_2 L_2}{2D_2}\left(\dfrac{D_1}{D_2}\right)^4\right]$	$\dfrac{A_r^2}{H}\left[\dfrac{f_1 L_1}{2D_1} - \dfrac{f_2 L_2}{2D_2}\left(\dfrac{D_1}{D_2}\right)^4\right]$
Φ_2	0	0	0	$\dfrac{A_r^2}{H}\left[\dfrac{f_2 L_2}{2D_2}\left(\dfrac{D_1}{D_2}\right)^4\right]$
M_1	$\dfrac{A_r^2}{H}\theta_1$	$-\dfrac{A_r^2}{H}\theta_2$	$\dfrac{A_r^2}{H}\left[\theta_1 - \theta_2\left(\dfrac{D_1}{D_2}\right)^4\right]$	$\dfrac{A_r^2}{H}\left[\theta_1 - \theta_2\left(\dfrac{D_1}{D_2}\right)^4\right]$
M_2	0	0	0	$\dfrac{A_r^2}{H}\theta_2\left(\dfrac{D_1}{D_2}\right)^4$
Q	$\dfrac{\bar{V}_1}{\bar{V}_{10}}$	$\dfrac{\bar{V}_2}{\bar{V}_{20}}$	$\dfrac{\bar{V}_1}{\bar{V}_{10}}$	$\dfrac{\bar{V}_1}{\bar{V}_{10}}$
ΔP	$\dfrac{\bar{P}_1 - P_{amb}}{\rho \bar{V}_{10}^2}$	$\dfrac{P_{amb} - \bar{P}_2}{\rho \bar{V}_{20}^2}$	$\dfrac{\bar{P}_1 - \bar{P}_2}{\rho \bar{V}_{10}^2}$	$\dfrac{\bar{P}_1 - \bar{P}_2}{\rho \bar{V}_{10}^2}$

Fig. 5 Schematic of experimental apparatus

pressure headers) to obtain uniform discharge flows in the laterals. The flow equations were then transposed by straightforward analytical methods (since the header velocity is now a linear function of distance) to obtain values of the momentum coefficients and effective friction factors for each header. The following coefficient data was obtained from the uniform flow tests:

$$\theta_1 = 1.05 \pm 0.05 \qquad (29)$$

$$\theta_2 = 2.60 \pm 0.05 \qquad (30)$$

This result is in agreement with the experimental values predicted in references [18 and 27]. The friction factors were in agreement with the Moody charts for smooth tubes using the Blasius correlation for which the friction factor varies with Reynolds number to the $(-1/4)$ power. The effects of the lateral penetrations through the walls of the headers in increasing the the friction factor could not be detected from the data.

Case A—Large Area Ratio and Large Lateral Resistance Manifold. The results of experiments for systems with an area ratio, A_r, of 2.810 and a lateral flow resistance, H, of 12.2 lateral velocity heads (2.54 cm diameter orifice) are presented in Figs. 6(a) and 6(b). There are 20 branch points along each header. The ordinate for each figure is the dimensionless distance, x_1/L_1, from the entrance of the dividing flow header. Three data sets are shown on each figure. The pressures in each header are plotted as multiples of a reference pressure, ΔP_r, which is defined as the pressure differential between the inlet to the dividing flow header and the outlet from the combining flow header. For parallel flow, $\Delta P_r = \bar{P}_1(0) - \bar{P}_2(1)$. For reverse flow, $\Delta P_r = \bar{P}_1(0) - \bar{P}_2(0)$. The third data set illustrates the local pressure difference between headers as normalized with respect to the maximum pressure difference between headers, $(P_1(x) - P_2(x))_{max}$. The third curve can be interpreted as a measure of the relative discharge flow since the flow rate in the laterals is proportional to the square root of the differential pressure between headers.

Since the dividing flow header is dominated by the effects of static pressure regain due to branching (i.e., small friction effects), the pressure characteristics of each header are better matched to provide a more uniform discharge for the reverse flow system than for the parallel flow system. Note that the only difference between these two manifolds is the orientation of the outlet.

Case B—Large Area Ratio and Small Lateral Resistance Manifold. The headers of the system described by Case A were separated and an orifice of diameter 3.18 cm was inserted in the laterals, giving a reduced flow resistance of 4.5 lateral velocity heads. The
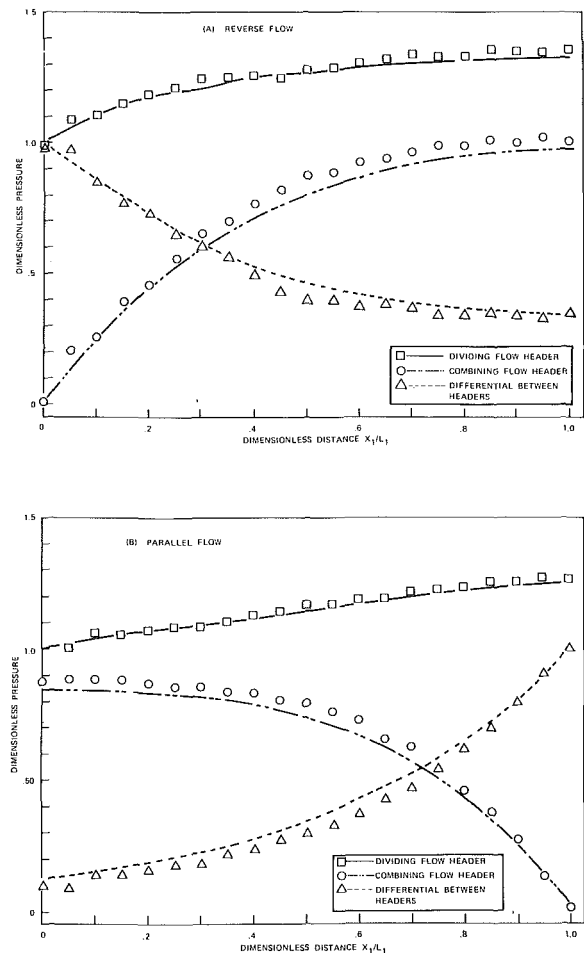

Fig. 6 Pressure profiles for manifolds with a large area ratio and large lateral resistance
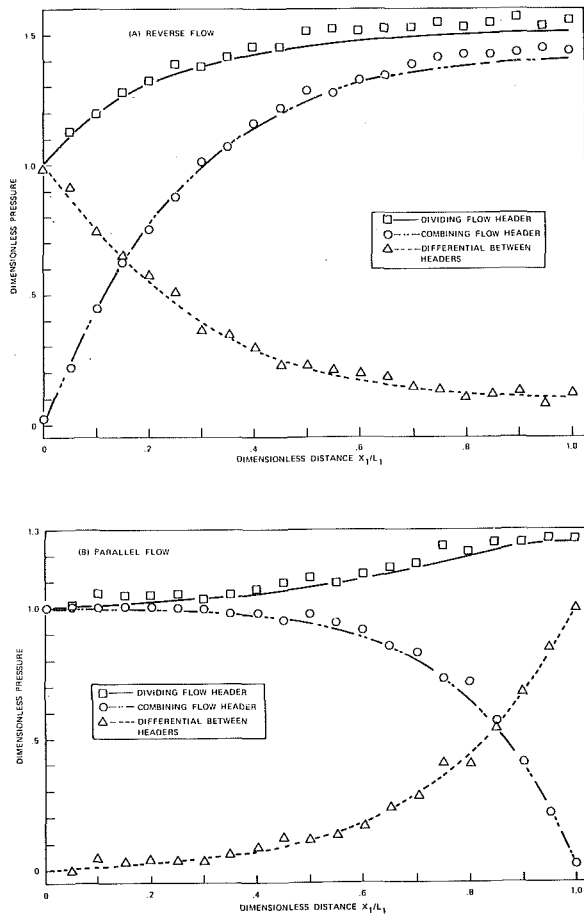
Fig. 7 Pressure profiles for manifolds with a large area ratio and small lateral resistance

Fig. 8 Pressure profiles for manifolds with a small area ratio and large lateral resistance

data for these experimental runs are presented in Figs. 7(a) and 7(b). The reduction of the lateral flow resistance brings about a poorer flow distribution for each system; however, the reverse flow manifold still exhibits a better flow balance due to the matched pressure characteristics of each header. For the parallel flow manifold, the differential pressure near $x = 0$ is almost zero and little discharge occurs in this region.

Case C—Small Area Ratio and Large Lateral Resistance Manifold. The length of the headers described above was reduced by 50 percent and tests were conducted for systems with 10 laterals. Case C represents a system with an area ratio of 1.405 and a lateral resistance of 12.2. This system is identical to Case A except for the shortened headers. The data are presented on Figs. 8(a) and 8(b). The flow distribution is nearly uniform due to the large flow resistance of the laterals and the small area ratio.

Case D—Small Area Ratio and Small Lateral Resistance Manifold. The manifold of Case C was altered to obtain a flow resistance of 4.5 velocity heads in the laterals by the insertion of the larger orifice. The data for these experiments are presented in Figs. 9(a) and 9(b). The flow distribution is poorer than Case C due to the smaller lateral resistance.

Comparison With Analytical Model. The curves on Figs. 6 through 9 illustrate the pressure profiles predicted by the analytical model. Table 4 lists the values of the parametric coefficients of the pressure-flow equations for each system. All curves are normalized with respect to the reference pressure conditions described above. In programming the computer solutions, the following assumptions were made. First, the friction factors were
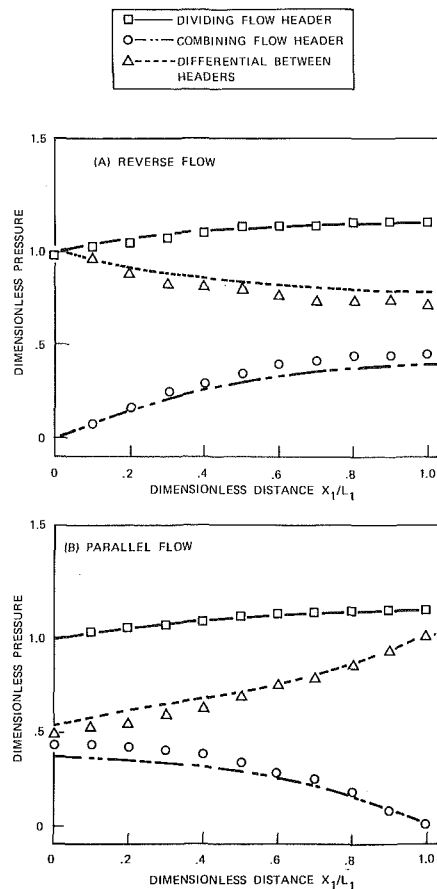
allowed to vary with Reynolds number and were calculated based on the smooth tube correlation. The exponent, n, used for friction factor variations was $(-1/4)$. Second, allowances were made for variations in the momentum coefficient θ_1 to account for a readjustment of the velocity profile in the neighborhood of the first few laterals in the dividing flow header. From the data of references [18 and 27], the value of θ_1 for laterals with infinite spacing is taken as 1.30 and is reduced to 1.05 as the spacing between laterals is decreased. The computations were carried out with a linear variation of θ_1 from 1.30 to 1.05 over the dimensionless distance, x, from 0.0 to 0.2. The value of θ_1 was assumed constant for the remainder of the manifold. Third, a value of $d\beta_1/dx$ of (-0.3) was included in the computations for the dimensionless distance, x, from 0.0 to 0.2. It was observed that the pressure data for the dividing flow header suffered an abrupt increase near the entrance and then slowly increased toward the dead end of the header. (Refer to Fig. 6(a), for ex-

TABLE 4 COEFFICIENTS OF THE PRESSURE-FLOW
EQUATION SET FOR FIGURES 6 - 9

Figure	A_1	A_2	B_1	B_2	Z
6A	0.81	0	-1.55	0	1.14
6B	0.40	0.40	1.05	2.60	1.14
7A	0.81	0	-1.55	0	1.88
7B	0.40	0.40	1.05	2.60	1.88
8A	0.40	0	-1.55	0	0.57
8B	0.20	0.20	1.05	2.60	0.57
9A	0.40	0	-1.55	0	0.94
9B	0.20	0.20	1.05	2.60	0.94

Fig. 9 Pressure profiles for manifolds with a small area ratio and small lateral resistance
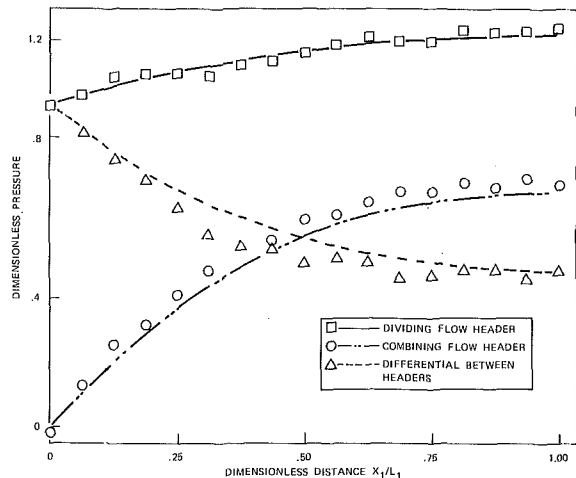

Fig. 10 Pressure profiles for the last 80 percent of a reverse flow manifold with large area ratio and large lateral resistance (reference Fig. 6(a))

decay of the entrance disturbance indicated that a value of -0.2 should be used for $d\beta_1/dx$; however, the value of -0.3 above provided the best fit to the experimental data.

The above entrance conditions are relevant only to the presene experimental configuration. Therefore, the adjustments madt in the momentum coefficient β_1 are not considered to be of general applicability. The complications of the distorted entrance velocity profile can be removed from the experimental data, however, by analyzing only the portion of the manifold downstream from the entrance where the velocity profile has adjusted to a fully developed condition. Computer solutions for each of the manifolds described in Figs. 6 through 9 were obtained for a portion of the original manifolds corresponding to the distance interval from $x = 0.2$ to the end of the header (i.e., the last 80 percent of the headers). In these computations, the fully developed value of $\theta_1 = 1.05$ was used and the momentum term $d\beta_1/dx$ was taken to be zero. The agreement of the analytical model for fully developed flow with the shortened manifolds is illustrated by Figs. 10 and 11. Fig. 10 is related to Fig. 6(a) and Fig. 11 is related to Fig. 7(b). The agreement between the analytical solutions and the experimental data is good. Fig. 12 is

ample.) This increase in pressure at the entrance to the dividing flow header was attributed to a nonsymmetrical velocity profile present in the neighborhood of the first few laterals. The velocity profile distortion resulted from the sum total of the following effects. Air drawn through the manifold system by the blower was recirculated in the laboratory to maintain a constant air temperature. These recirculation currents from the blower exhaust air would cause random vorticity to be present in the intake air stream of the dividing flow header, which consisted of only a sharp-edged, short length of pipe with no other ductwork or calming sections. (Limitations on the laboratory space available prohibited the construction of a smoother entrance section.) Distortion in the entrance flow was verified by velocity rake profiles, which were nonsymmetrical at the measuring cross-section. This initial distortion was further accentuated by the tygon tubing behind the velocity rake support which was used to transmit the total pressure to a manometer tube bank. While distortion in the entrance velocity profile is undesirable from an academic viewpoint, nonuniform entrance conditions are typically found in many industrial manifold designs. Therefore, the present experiments may be viewed as a realistic test of the analytical model.

Computer solutions were obtained for various values of the friction factor, the momentum coefficients θ_1 and θ_2, and the velocity profile adjustment factor $d\beta_1/dx$. The computer solutions could not be adjusted to account for the jump in pressure at the entrance to the dividing flow header without the inclusion of the $d\beta_1/dx$ term, even for wide ranges in the values of the other momentum coefficients and the friction factors. It was, therefore, concluded that the adjustment of the entrance velocity profile to a fully developed condition is a significant factor affecting the flow distribution in a manifold. Analytical calculations for the
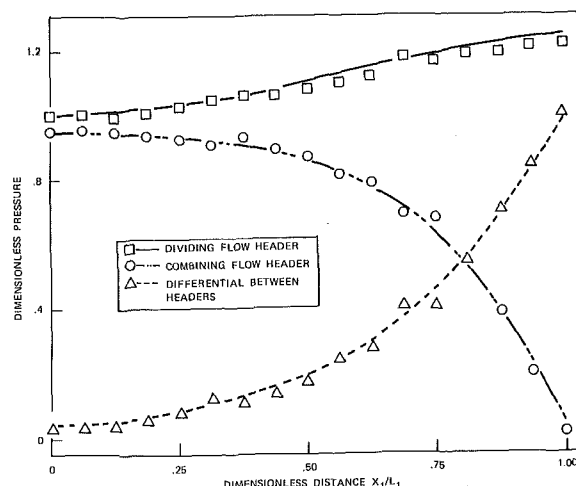

Fig. 11 Pressure profiles for the last 80 percent of a parallel flow manifold with large area ratio and small lateral resistance (reference Fig. 7(b))

Transactions of the ASME

taken from reference [18] and illustrates the application of the fully developed flow concept described here to the last 16 laterals (out of 20) for a simple dividing flow manifold.

No adjustment was applied to the combining flow headers to account for variations in the momentum coefficient β_2 since the velocity is nearly zero at stations in the combining flow header where changes in β_2 would be greatest. Hence, the correction would contribute negligible pressure change (locally) in the computer solutions. This procedure is supported by the agreement of the predictions of the analytical model with the data for a simple combining flow header taken from reference [18] as shown in Fig. 13. The value of $\theta_2 = 2.66$ used in the calculation was taken from the data of references [4 and 18].

Discussion

The data and analytical model presented above were developed for the case of a system with uniform areas and lateral resistances. Some general conclusions relevant to the performance of manifold systems can be illustrated with respect to these examples.

Parameters Affecting Flow Distribution. The pressure-flow equations and the flow distribution equation were presented in terms of dimensionless coefficients which were functions of many independent variables. These equations show that uniform flow distribution in the laterals is attained only when the headers act as infinite reservoirs. The infinite reservoir condition is approached when the dimensionless coefficients of the flow distribution equation approach zero. The individual variables comprising these coefficients affect the flow distribution in the following manner.

Area Ratio. The square of the area ratio, A_r^2, appears in the numerator of each term in the flow distribution equation. Hence, a large area ratio contributes to flow maldistribution in the manifold system since the value of the dimensionless coefficients is rapidly increased as the area ratio increases. A common design rule-of-thumb is to limit the area ratio to values less than one. The area ratio is also viewed as the porosity of the header.

Lateral Flow Resistance. The lateral flow resistance, H, appears in the denominator of each term in the flow distribution equation. Therefore, the value of the dimensionless coefficients decreases as the lateral flow resistance increases. An infinite flow resistance would cause even a small diameter header with large porosity to act as an infinite reservoir. Hence, large lateral resistance is desirable for good flow distribution. However, large lateral resistances result in a high total pressure loss for the manifold system which may be unacceptable if pumping costs are an important design consideration.

Length/Diameter Ratio. The relative length of a header enters the governing equations only through the friction terms. For headers of relatively small length/diameter ratio, the effects of friction may be neglected and the flow distribution equation can then be solved analytically. For relatively long headers, the effects of flow branching on the static pressure in the header can be neglected. Some analytical solutions for the flow distribution are also possible for friction dominated manifolds. Analytical solutions are discussed in references [18 and 27]. The effects of header length/diameter ratio must be separated from the area ratio effect for headers of constant porosity per unit length.

Momentum Parameters θ_1 and θ_2. The momentum parameters θ_1 and θ_2 are relatively fixed. The fully developed flow value of θ_1 is approximately 1.05 and is only weakly dependent on the ratio of diameters between the header and the laterals as shown by the data of various investigators [29]. The value of θ_2 becomes highly variable (see reference [27]) as the lateral/header diameter ratio increases to values of 0.5. However, most systems are de-

signed with lateral/header diameter ratios near 0.15 where θ_2 is nearly constant. Therefore the momentum parameters θ_1 and θ_2 cannot be considered as independent variables in a broad sense.

Diameter Ratios. The diameter ratio between headers in a reverse or parallel flow manifold will affect both the friction and momentum coefficients of the flow distribution equation as shown by Table 3. The momentum coefficients are more important in determining flow distribution than the friction coefficients. Therefore, a better flow distribution can be obtained by reducing the magnitude of the momentum coefficients by increasing the diameter of the combining flow header to offset the large value of the momentum parameter θ_2. Systems in which the dividing flow header is larger than the combining flow header will exhibit a poor distribution of flow in the laterals. The effect of variations in the header diameter ratio on the friction terms is not as great in altering the flow distribution. Changes in diameter ratio between the header and the laterals will not affect the flow distribution directly except through minor changes in the values of the lateral flow resistance coefficients, C_{TC} and C_{TD}, and the momentum term θ_2.

Momentum Parameter β. The momentum parameter β is necessary to account for variations in the velocity profile at the entrance to the manifold. The upstream history of the flow approaching the manifold and the design of the entrance (i.e., parallel or right angled impingement) determine the amount of velocity profile distortion present in a given system. Therefore the momentum parameter β cannot be generalized. As illustrated by the experiments reported in the present paper, one of the major factors contributing to the uncertainty in predicting the performance of a manifold is the entrance flow condition.

It has often been observed that a reversal of flow occurs in manifolds designed with out-of-plane bends leading to the entrance of the dividing flow header. Under these conditions, fluid can recirculate from the combining flow header into the dividing flow header through the laterals nearest the entrance. This effect has been demonstrated by Sherman [18] and LeRose (private communication) for similar entrance conditions. The momentum correction term $d\beta/dx$ in the governing equations is the only mechanism by which the flow reversal phenomenon can be explained analytically. For these poorly designed inlet conditions, the entrance pressure can be less than the pressure in the combining flow header of a parallel flow system. Therefore, fluid will be drawn into the dividing flow header. A pressure recovery will occur in the direction of flow due to the regain of pressure from the distorted entrance profile. Otherwise, the pressure is required to fall in the direction of flow as can be shown by a simple analysis of the governing equations. The experimental parallel flow systems reported above (Figs. 6(b) and 7(b)) could have exhibited a flow reversal in the first few laterals had the entrance to the dividing flow header been through a right angled bend rather than a straight inlet section. Flow reversal is more likely to occur in parallel flow manifolds which are subject to poor flow distribution since the differential pressure between headers is minimal at the entrance for these designs.

Friction Factor. The selection of a particular pipe material or surface finish will affect the value of the dimensionless friction coefficients in the governing equations. The present experimental results indicate that the friction factor can be calculated under the assumption that the branch points do not affect the friction pressure loss characteristics of the header. This conclusion is highly dependent on the spacing between laterals. Common design practice has been to evaluate the friction factor based on ordinary pipe friction calculations for the case of widely spaced branch points and to increase the value of the friction factor as the branch points become closely spaced. The present data indicate that a spacing of 6.8 lateral diameters may be taken as a case representative of widely spaced laterals.

Selection of Design Variables. The area ratio and the lateral flow resistance are the variables which most significantly affect the flow distribution in a manifold system. The effects of these two terms is clearly indicated in the experimental results reported by Figs. 6 through 9. In many system designs, the area ratio and lateral flow resistance are fixed by other requirements. Therefore, the only other design parameters which may be altered to improve flow distribution are the relative length of the manifold, the friction factors, and the orientation between the inlet and outlet headers. A reverse flow system will have a better flow distribution than a parallel flow system (other parameters the same) when the dividing flow header is dominated by pressure recovery due to branching and friction effects are minimal. A parallel flow system can give better flow distribution than a reverse flow system if friction effects dominate the dividing flow header (but this is not necessarily so). In general, the flow distribution in a reverse flow system will be better than the parallel flow system for most designs used in industrial applications. The total pressure losses for the reverse flow system are typically less than for the parallel flow system.

Application of Analytical Model. The analytical model has been formulated in terms of both a pressure-flow equation set and a flow distribution equation. The advantages of each system of equations may be summarized as follows. The pressure-flow equation set clearly shows the relationship between pressure and velocity changes in the headers and readily leads to a physical interpretation of the manifold problem. The formulation of the equations in terms of first derivative expressions for pressure and velocity allows for a variation of parameters like lateral resistance, porosity, and the momentum coefficients along the header, without the need to express these variations in terms of continuously differentiable functions. Therefore the pressure-flow set of equations can accept system designs in which the number of laterals at a branch point may vary discontinuously with axial location. The pressure-flow equation set is recommended for general computational use in determining the performance of a given manifold.

Alternatively, the flow distribution equation has the advantage of being formulated in terms of only one dependent parameter, namely the flow rate in the dividing flow header. This equation may be solved analytically under some conditions [27]. However, if the design of the manifold is not constant along the path length, then it is necessary to formulate functions such as dH/dx for lateral resistance, $d(A_r)/dx$ for the area ratio, etc., when these parameters vary with distance. Stepwise changes in these parameters are difficult to accommodate analytically since the derivatives become infinite. For systems in which manifold flow coefficients are constants, the performance of the manifold can be determined parametrically from the flow distribution equation (see reference [27]) for ease in design usage.

In addition to predicting the performance of a given design, the governing equations can be solved alternatively to predict the form of the lateral resistance variation along the headers necessary to give uniform flow distribution in the laterals. This design procedure can be accomplished by assuming that the dimensionless volume flow rate in a header is given by $(1-x)$. Then it is possible to solve for the local resistance at each value of (x) which satisfies the governing equations.

Many manifold systems are designed with multiple outlet headers and a single inlet header to improve flow distribution. Other designs use inlet arrangements which are not symmetrically spaced with respect to the outlet header. One example of such a design is illustrated by a system for which the inlet flow enters the dividing flow header at its midpoint and leaves the combining flow header at one of the ends. The calculation of the flow distribution in manifolds of this type is facilitated by the application of the proposed analytical model since the conservation of mass bookkeeping requirement is automatically satisfied by the governing equations. Analytical models for nonsymmetrical manifold designs are discussed in reference [29].

The analytical model is formulated in terms of the momentum equation as the governing conservation equation for the header flow streams. An alternative approach is to use the Bernoulli equation to compute the pressure changes in the headers as a result of the branching process. The dashed line on Fig. 12 illustrates the application of the Bernoulli equation (represented by $\theta_1 = 1.00$) to a simple dividing flow header. The momentum model using the value of $\theta_1 = 1.06$ clearly gives a better fit to the data. The data of Fig. 13, which illustrates the application of the momentum model to a simple combining flow manifold, could not be adequately represented by a solution utilizing the Bernoulli equation ($\theta_2 = 1.00$) to predict the pressure changes in the header due to branching. These two examples clearly demonstrate the superiority of momentum models over Bernoulli models for branching process.

Summary

The analytical model for flow distribution in manifolds described in the present paper was formulated from a first principles approach to the problem which included the use of the continuity and momentum equations for the header flows and a discharge equation for the lateral flows. The approach has been generalized in terms of dimensionless equations and flow coefficients. The model is applicable to a wide range of system designs. The experimental results are in substantial agreement with the analytical model. The analytical model is recommended for general application in the analysis of flow distribution in manifolds.
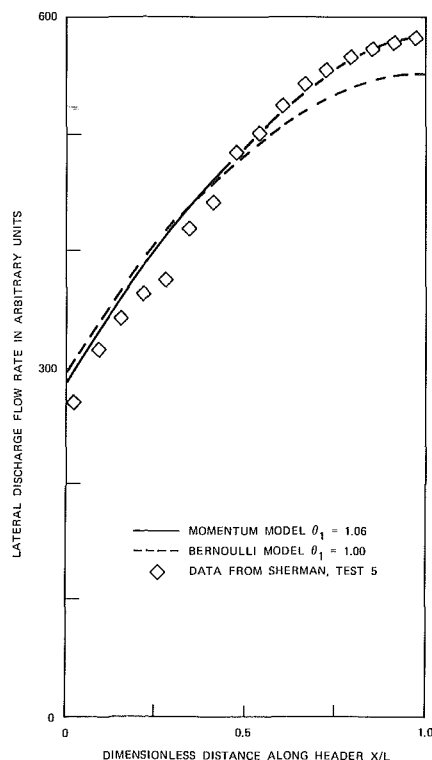
Acknowledgments

Fig. 12 Comparison of analytical model with experimental data for a simple dividing flow manifold with large area ratio and small lateral resistance (reference [18])

(Figure legend:)
——— MOMENTUM MODEL θ_1 = 1.06
– – – BERNOULLI MODEL θ_1 = 1.00
◇ DATA FROM SHERMAN, TEST 5

Y-axis: LATERAL DISCHARGE FLOW RATE IN ARBITRARY UNITS (0, 300, 600)
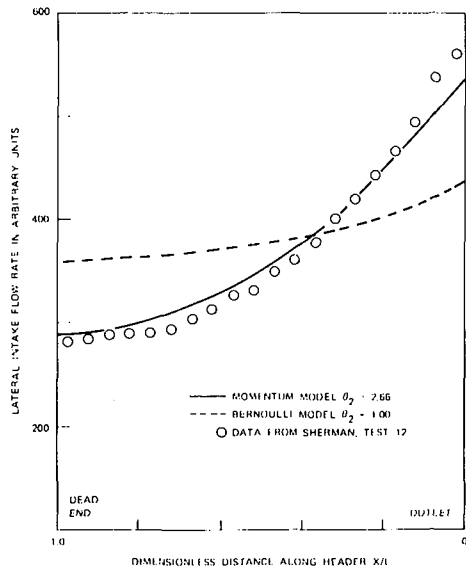X-axis: DIMENSIONLESS DISTANCE ALONG HEADER X/L (0, 0.5, 1.0)

Fig. 13 Comparison of analytical model with experimental data for a simple combining flow manifold with large area ratio and large lateral resistance (reference [18])

Part of the numerical computations were carried out at the West Virginia University Computer Center under a faculty research grant.

References

1 McNown, J. S., "Mechanics of Manifold Flow," *Transactions ASCE*, Vol. 119, 1954, pp. 1103–1142.

2 McNown, J. S., and Hsu, E. Y., "Application of Conformal Mapping to Divided Flow," *The First Midwestern Conference on Fluid Dynamics*, May 12–13, 1950, at the University of Illinois, pp. 143–155, 1951.

3 Zeisser, M. H., "Summary Report of Single-Tube Branch and Multi-Tube Branch Water Flow Tests Conducted by the University of Connecticut," Pratt and Whitney Aircraft Division, United Aircraft Corporation, *Report No. PWAC-231*, USAEC Contract AT (11-1)-229, May 1963.

4 Starosolszky, O., "Pressure Conditions in Pipe Branches," *Vizugyi Kozlemenyek* (Budapest) No. 1, pp. 115–121, 1958. (Translated by Language Service Bureau, Washington, D.C., on file at the Agricultural Research Service, St. Anthony Falls Hydraulic Laboratory, Minneapolis, Minn.)

5 Ruus, E., "Head Losses in Wyes and Manifolds," *Journal of the Hydraulics Division, ASCE*, Vol. 3, Mar. 1970, pp. 593–608.

6 Kubo, T., and Ueda, T., "On the Characteristics of Divided Flow and Confluent Flow in Headers," *Bulletin of JSME*, Vol. 12, No. 52, 1969, pp. 802–809.

7 Kubo, T., and Ueda, T., "On the Characteristics of Confluent Flow of Gas-Liquid Mixtures in Headers," *Bulletin of JSME*, Vol. 16, No. 99, 1973, pp. 1376–1384.

8 Oakey, J. A., "Hydraulic Losses in Short Tubes Determined by Experiments," *Engineering News Record*, June 1, 1933, pp. 717–718.

9 Koh, R. C. Y., and Brooks, N. H., "Fluid Mechanics of Waste-Water Disposal in the Ocean," *Annual Review of Fluid Mechanics*, Vol. 7, 1975, pp. 187–211, Annual Reviews, Inc., Palo Alto, Calif.

10 Acrivos, A., Babcock, B. D., and Pigford, R. L., "Flow Distribution in Manifolds," *Chemical Engineering Science*, Vol. 10, No. 1/2, 1959, pp. 112–124.

11 Keller, J. D., "The Manifold Problem," *Journal of Applied Mechanics*, TRANS. ASME, Vol. 71, Mar. 1949, pp. 77–85. (Discussion in TRANS. ASME, Vol. 71, Sept. 1949, pp. 320–322.)

12 Dow, W. M., "The Uniform Distribution of a Fluid Flowing Through a Perforated Pipe," *Journal of Applied Mechanics*, TRANS. ASME, Vol. 72, Dec. 1950, pp. 431–438. (Discussion in TRANS. ASME, 1951, Vol. 73, pp. 221–224.)

13 Dittrich, R. T., "Experimental Study of Flow Distribution and Pressure Loss with Circumferential Inlet and Outlet Manifolds," NASA Technical Note TN D-6697, Mar. 1972.

14 Enger, M. L., and Levy, M. I., "Pressures in Manifold Pipes," *Journal of the American Water Works Association*, May 1929, pp. 659–667.

15 Van der Hegge Zijnen, B. G., "Flow Through Uniformly Tapped Pipes," *Applied Science Research*, Vol. A3, 1952, pp. 144–162.

16 Markland, E., "Analysis of Flow from Pipe Manifolds," *Engineering*, Vol. 187, Jan. 30, 1959, pp. 150–151.

17 Soucek, E., and Zelnick, E. W., "Lock Manifold Experiments," *Trans. ASCE*, 1945, pp. 1357–1400.

18 Bajura, R. A., "A Model for Flow Distribution in Manifolds," *Journal of Engineering for Power*, TRANS. ASME, Vol. 93, 1971, pp. 7–12.

19 Howland, W. E., "Design of Perforated Pipe for Uniformity of Discharge," *Proceedings of the Third Midwest Conference on Fluid Mechanics*, 1953, pp. 687–701.

20 Pearlmutter, M., "Inlet and Exit Header Shapes for Uniform Flow Through a Resistance Parallel to the Main Stream," *Journal of Basic Engineering*, TRANS. ASME, Vol. 83, Sept. 1961, pp. 361–370.

21 Mardon, J., Hauptmann, E. G., Monahan, R. E., and Brown, E. S., "The Extant State of the Manifold Problem," Technical Paper T346, *Pulp and Paper Magazine of Canada*, Nov. 1971, v. 72, n. 11.

22 Haerter, A. A., "Flow Distribution and Pressure Change Along Slotted or Branched Ducts," *ASHRAE Journal*, Vol. 5, Jan. 1963, pp. 47–59.

23 Horlock, J. H., "An Investigation of the Flow in Manifolds with Open and Closed Ends," *Journal of the Royal Aeronautical Society*, Vol. 60, Nov. 1956, pp. 749–753.

24 Olsen, F. C. W., "Flow Through a Pipe with a Porous Wall," *Journal of Applied Mechanics*, TRANS. ASME, Vol. 71, Mar. 1949, pp. 53–54. (Discussion in TRANS. ASME, Sept. 1949, Vol. 71, pp. 317–318.)

25 Huang, J. C. P., and Yu, H. S., "Pressure Distributions in Porous Ducts of Arbitrary Cross Section," ASME Paper 73-FE-9, Presented at the ASME Joint Applied Mechanics-Fluids Engineering Conference, Atlanta, Ga., June 20–22, 1973.

26 Quaile, J. P., and Levy, E. K., "Laminar Flow in a Porous Tube With Suction," ASME Paper 73-WA/HT-1, Presented at the ASME Winter Annual Meeting, Detroit, Mich., November 11–15, 1973.

27 Bajura, R. A., LeRose, V. F., and Williams, L. E., "Fluid Distribution in Combining, Dividing and Reverse Flow Manifolds," ASME Paper 73-PWR-1, Presented at the ASME-IEEE Joint Power Generation Conference, New Orleans, La. September 16–19, 1973.

28 Jones, E. H., Jr., "Pressure and Flow Distribution in a Manifold," MS thesis, Department of Mechanical Engineering and Mechanics, West Virginia University, Morgantown, West Va., May 1974.

29 LeRose, V. F., "An Analytical Study of Flow Distribution in Manifolds," MS thesis, Department of Mechanical Engineering, West Virginia University, Morgantown, West Va., May 1972.